

Optimization analysis of an endoreversible quantum heat engine with efficient power function

Kirandeep Kaur,^{1,*} Anmol Jain,² Love Sahajbir Singh,² Rakesh Singla,³ and Shishram Rebari^{3,†}

¹*Department of Physical Sciences, Indian Institute of Science Education and Research Mohali, Sector 81, S.A.S. Nagar, Manauli PO 140306, Punjab, India*

²*Department of IT, Dr B R Ambedkar National Institute of Technology Jalandhar, Punjab-144027, India*

³*Department of Physics, Dr B R Ambedkar National Institute of Technology Jalandhar, Punjab-144027, India*

We study the optimal performance of an endoreversible quantum dot heat engine, in which the heat transfer between the system and baths is mediated by qubits, operating under the conditions of a trade-off objective function known as maximum efficient power function defined by the product of power and efficiency of the engine. First, we numerically study the optimization of the efficient power function for the engine under consideration. Then, we obtain some analytic results by applying high-temperature limit and compare the performance of the engine at maximum efficient power function to the engine operating in the maximum power regime. We find that the engine operating at maximum efficient power function produces at least 88.89% of the maximum power output while at the same time reduces the power loss due to entropy production by considerable amount. We conclude by studying the stochastic simulations of the efficiency of the engine in maximum power and maximum efficient power regime. We find that the engine operating at maximum power is subjected to less power fluctuations as compared to the one operating at maximum efficient power function.

I. INTRODUCTION

Back in 1824, Sadi Carnot proposed an ideal thermodynamic cycle, known as Carnot cycle, working between two reservoirs at different temperatures T_c and T_h ($T_c < T_h$) to convert heat into work. The efficiency of Carnot cycle, $\eta_C = 1 - T_c/T_h$, is a universal result. However, due to its reversible nature, it takes infinite time to complete one Carnot cycle, thereby producing vanishing power output per cycle. However, realistic engines should work under irreversible conditions by taking into account the finite-time constraints and produce finite-power output [1–3]. In search for optimizing the performance of realistic heat engines, the field of finite-time thermodynamics was developed [2–6]. Curzon-Albhorn (CA) were the pioneers of the finite-time thermodynamic and they introduced a simple Carnot-like heat engine model, known as endoreversible model [1, 7], in which irreversible heat transfer between the working medium and the reservoirs is assumed to obey Newton's law of conduction [1]. The efficiency of endoreversible at maximum power is given by

$$\eta_{CA} = 1 - \sqrt{1 - \eta_C} = \frac{\eta_C}{2} + \frac{\eta_C^2}{8} + \frac{\eta_C^3}{16} + \dots \quad (1)$$

As in the case of the Carnot efficiency, the CA efficiency depends on the ratio of reservoir temperatures only. The endoreversible model has paramount importance in the field of finite-time thermodynamics as many different models of heat engines, working under the conditions of maximum power [8–14], share the universality

of efficiency up to the second order term in η_C [8, 15] with CA efficiency.

Over the past few decades, the technological advanced made it possible to manipulate quantum systems operating at nanoscale [16–21]. Since the size and quantum effects play an important role in thermodynamic properties of the system, the extension of the theory of classical thermodynamics to the quantum systems is called for [22–27]. Quantum heat engines, being the technological devices of practical importance, provide us with ideal platform to study the relation between classical and quantum thermodynamics [28–30].

Further, the rapid development in the field of quantum technologies has bring up the question of resource consumption in the thermodynamic landscape [31]. The heat engines working at maximum power regime are also known to waste a large amount of fuel due to large amount of entropy production, which pollutes the environment in turn [5, 32]. Thus taking into account the ecological and economical concerns, one should operate heat engines in such a regime which establishes a compromise between the efficiency and power of the heat engine [5, 32–40]. Efficient power function is such an alternative trade-off objective function which is defined by the product of efficiency and power of the heat engine [41], thus taking caring of the compromise between power and efficiency. It was introduced by Stucki to study the biochemical energy conversion process [41]. Over the past three decades, it has been successfully used in studying the energy conversion process in classical [42–49] as well as quantum thermal devices [50, 51].

In this work, we study the optimal performance of a quantum endoreversible model [52, 53], in which heat transfer between the working fluid and the reservoirs is mediated by qubits, working under the conditions of maximum efficient power function. Unlike the classical

* kiran.nitj@gmail.com

† rebaris@nitj.ac.in

endoreversible heat engine, the laws of heat transfer no longer obey the Newton's law of conduction and filtration of the heat current through the quantum qubits introduces the quantum effects in the performance of the quantum version of endoreversible engine.

The paper is organized as follows. In Sec. I we introduce the model of quantum endoreversible heat engine. In Sec III we numerically optimize the performance of the engine and present our result. In Sec IV, we restrict ourselves to the high-temperature limit and compare the performance of the heat engine at maximum efficient power to the engine at maximum power. Sec. V is devoted to study of the stochastic fluctuations in the power output of the the engine. We conclude in Sec. VI.

II. MODEL AND THEORY

The schematics of the quantum version of the endoreversible engine is shown in Fig. 1. During the hot isothermal branch, the qubits 1, with energy gap E_1 , induces the irreversible heat flux Q_1 from the thermal bath at temperature T_h to the working fluid at temperature T_1 . Similarly, during the cold isothermal branch, heat flux Q_2 from the working fluid at temperature T_2 to the cold reservoir at temperature T_c is mediated via qubit 2 having energy gap E_2 . The model in Fig. 1 will operate as an heat engine provided the following condition is satisfied: $T_h \geq T_1 \geq T_2 \geq T_c$.

The hamiltonian of the k ($k = 1, 2$) qubit is given as:

$$\hat{H}_k = \frac{E_k}{2} \hat{\sigma}_k^z, \quad (2)$$

and

where $\hat{\sigma}_k^z$ is third component of spin- $\frac{1}{2}$ Pauli matrix. The dynamics of the qubit 1 (2) is governed by the following master equation

$$\dot{\rho}_{1(2)} = -i[\hat{H}_{1(2)}, \rho_{1(2)}] + D_{h(c)}[\rho_{1(2)}] + D_{1(2)}[\rho_{1(2)}], \quad (3)$$

where the $D_{h(c)}[\rho_{1(2)}]$ and $D_{1(2)}[\rho_{1(2)}]$ are the Lindblad superoperators associated with baths of temperature of $T_{h(c)}$ and $T_{1(2)}$, respectively. The form of these Lindblad dissipators for the qubit 1 is given by the following equation:

$$D_i[\rho_1] = \Gamma_i(n_i + 1) \left[\sigma_1^- \rho_1 \sigma_1^+ - \frac{1}{2} \{ \sigma_1^+ \sigma_1^-, \rho_1 \} \right] + \Gamma_i n_i \left[\sigma_1^+ \rho_1 \sigma_1^- - \frac{1}{2} \{ \sigma_1^- \sigma_1^+, \rho_1 \} \right], \quad (4)$$

where $i = 1, h$ denote baths of temperature T_1 and T_h , respectively. Γ_i denotes the dissipation rate associated with bath i . Similarly, for the qubit 2, we have

$$D_j[\rho_2] = \Gamma_j(n_j + 1) \left[\sigma_2^- \rho_2 \sigma_2^+ - \frac{1}{2} \{ \sigma_2^+ \sigma_2^-, \rho_2 \} \right] + \Gamma_j n_j \left[\sigma_2^+ \rho_2 \sigma_2^- - \frac{1}{2} \{ \sigma_2^- \sigma_2^+, \rho_2 \} \right], \quad (5)$$

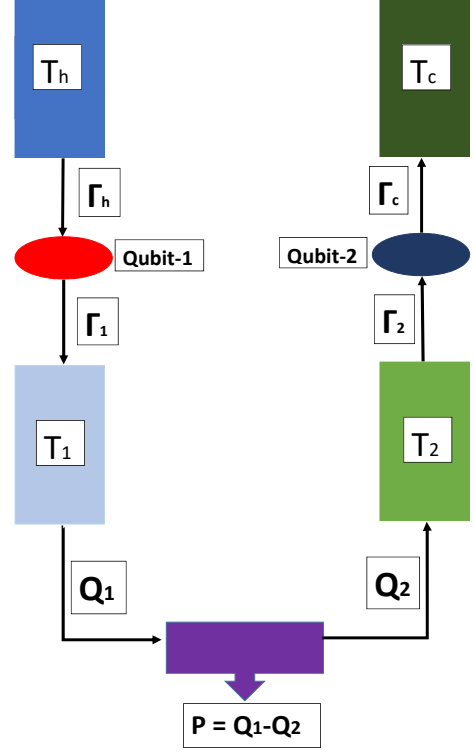


FIG. 1. The schematic diagram of quantum dot heat engine with irreversible heat transfer. In this model we have two qubits (1 and 2) which interact with the two bath. The location of qubit 1 is in between the hot bath (T_h) and working medium. The temperature of qubit 1 is denoted by T_1 . In the similar way qubit 2 is located in between the cold bath (T_c) and working medium. The temperature of qubit 2 is denoted by T_2 . The coupling strength of qubit 1 with hot bath and working medium is, Γ_h and Γ_1 respectively. In the similar way the coupling strength of qubit 2 with cold bath and working medium is Γ_c and Γ_2 respectively. E_1 and E_2 represents the energy level value of qubit 1 and qubit 2 respectively.

where $j = 2, c$ for baths of temperature T_2 and T_c respectively. $\sigma_k^+ = |1 \rangle \langle 0|$ and $\sigma_k^- = |0 \rangle \langle 1|$ are raising and lowering operators for the qubit k ($k = 1, 2$), respectively. $n_{i(j)} = 1/(e^{E_1(2)/k_B T_i(j)})$ is the number of photons in the reservoir i (j) with energy gap $E_1(2)$, where $i = 1, h$ and $j = 2, c$. From now on, we put $k_B = 1$.

In the steady state, the populations of qubit 1 can be obtained by setting $\dot{\rho}_1 = 0$ in the left hand side of Eq. (3). Thus, we have

$$\rho_1^s = \frac{1}{2}(1 + a_1^z \sigma_1^z), \quad (6)$$

where $a_1^z = -(\Gamma_h + \Gamma_1)/(\Gamma_1(2n_1 + 1) + \Gamma_h(2n_h + 1))$. In steady state, the heat flux $Q_h = Tr(H_1 D_h[\rho_1^s])$ flowing out of the heat bath at T_h is equal to the heat flux $Q_1 = -Tr(H_1 D_1[\rho_1^s])$ entering bath 1 at temperature T_1 . The

final expression for the heat flux Q_1 absorbed by the engine is given by

$$Q_1 = \gamma_1 E_1 (n_h - n_1), \quad (7)$$

where $\gamma_1 = (\Gamma_h + \Gamma_1)/(\Gamma_1(2n_1 + 1) + \Gamma_h(2n_h + 1))$. Similarly, the expression for the heat flux Q_2 rejected to cold reservoir at temperature T_c is given by

$$Q_2 = \gamma_2 E_2 (n_2 - n_c), \quad (8)$$

where $\gamma_2 = (\Gamma_c \Gamma_2)/(\Gamma_2(2n_2 + 1) + \Gamma_c(2n_c + 1))$.

By using Eqs. (7) and (8), we can obtain expressions for the power output and efficiency of the engine:

$$\begin{aligned} P &= Q_1 - Q_2, \\ &= \gamma_1 E_1 \left[\frac{1}{e^{E_1/T_h} - 1} - \frac{1}{e^{E_1/T_1} - 1} \right] \\ &\quad - \gamma_2 E_2 \left[\frac{1}{e^{E_2/T_2} - 1} - \frac{1}{e^{E_2/T_c} - 1} \right], \end{aligned} \quad (9)$$

and

$$\eta = \frac{P}{Q_1} = 1 - \frac{\gamma_2 E_2 (n_1 - n_c)}{\gamma_1 E_1 (n_h - n_1)}. \quad (10)$$

Further, for an endoreversible heat engine, the entropy productions of the working medium in two isothermal processes satisfy the following relation

$$\frac{Q_1}{T_1} = \frac{Q_2}{T_2}, \quad (11)$$

and the efficiency of the engine depends on internal temperatures of the working fluid during the isotherms:

$$\eta = 1 - \frac{T_2}{T_1}. \quad (12)$$

By using Eqs. (10), (11) and (12), we get the relations between the temperatures T_1 and T_2 and the efficiency (η) as follows (see Ref. [1] for details)

$$T_1 = \frac{E_1}{\ln \left[\frac{1}{n_h - \frac{Q_2}{\gamma_1 E_1 (1-\eta)}} + 1 \right]}, \quad T_2 = \frac{E_2}{\ln \left[\frac{1}{n_c + \frac{Q_1(1-\eta)}{\gamma_2 E_2}} + 1 \right]}. \quad (13)$$

III. OPTIMIZATION OF EFFICIENT POWER FUNCTION

The optimization of power output of the quantum endoreversible engine has already been studied in Ref. [52]. Here, we would like to study the optimal performance of endoreversible quantum heat engine operating at maximum efficient power function, which is more suitable objective function to optimize we if want to operate our engine in such a regime which pay equal attention to both efficiency and power of the engine. The expression for the efficient power function ($P_\eta = \eta P$), simply given

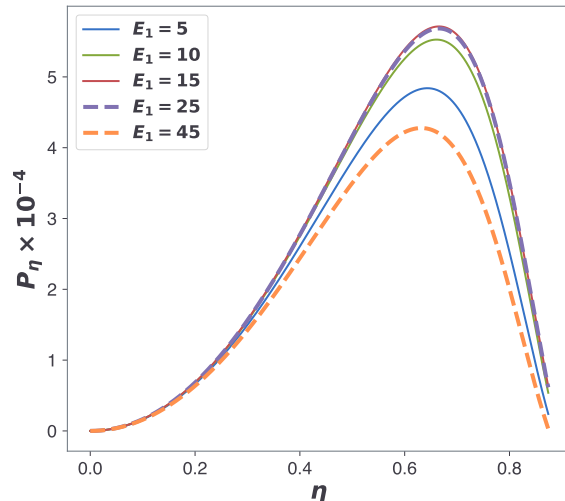


FIG. 2. Plot of the efficient power function (Eq. (14)) as a function of efficiency (η) of the engine for different set of values of $E_1 = 5, 10, 15, 25$, and 45 . The other parameters are fixed at constant values. $E_2 = 6$, $\Gamma_h = \Gamma_1 = 0.01$, $\Gamma_c = \Gamma_2 = 0.001$, $T_h = 10$, $T_c = 1$.

by the product of power and efficiency of the engine, can be obtained by combining Eqs. (9), (10), (11) and (12), and is given by

$$P_\eta = \frac{\gamma_2 E_2 \eta^2}{1 - \eta} \left\{ \frac{1}{\left[\frac{1}{n_h - P/(\gamma_1 E_1 \eta)} \right]^{E_2/E_1(1-\eta)} - 1} - n_c \right\}. \quad (14)$$

Now, we will optimize the efficient power function given in Eq. (14) by using numerical techniques. Figs. 2 and 3 show the efficient power function varying with efficiency η for different sets of values of E_1 and E_2 , respectively. The trends in both figures are same. It is observed that if we increase the value of E_1 and E_2 beyond a certain value, then the efficient power function decreases very fast. This can be explained by looking into the expressions for average number of photons with energy E_1 and E_2 in the reservoirs, which decreases with increasing energy gap $E_{1(2)}$. Then, it can be seen from Eqs. (7) and (8) that power output of the engine must be very small for very large E_1 or E_2 . On the other extreme, Eq. (9) indicates that power output will be vanishingly small for very small values of E_1 and E_2 . Thus, in order to optimize the performance of the engine, we have to tune the energy gaps (E_1 or E_2) somewhere in between the lower and higher values. Thus, we can claim that performance of the endoreversible quantum engine is affected by the properties of the qubits, which controls the irreversible heat transfer between the reservoirs and the working fluid. By adjusting the energy gaps of the qubits, we can regulate power and efficiency of the engine.

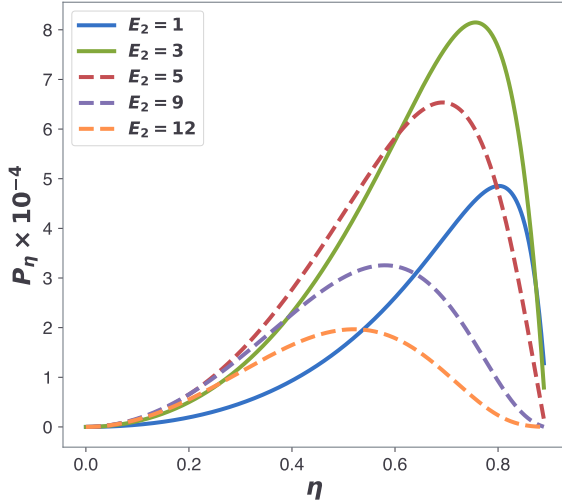


FIG. 3. Plot of the efficient power function (Eq. (14)) as a function of efficiency (η) of the engine for different set of values of $E_2 = 1, 3, 5, 9,$ and 12 . The other parameters are fixed at constant values. $E_2 = 6, \Gamma_h = \Gamma_1 = 0.01, \Gamma_c = \Gamma_2 = 0.001, T_h = 10, T_c = 1$.

In order to compare the performance of the engine operating at maximum efficient power function to the engine at maximum power, we plot Fig. 4. It is clear from Fig. 4 that the engine at maximum efficient power yields larger efficiency than the engine operating at maximum power. This is due to the fact that optimization of efficient power function, by definition, takes care of the trade-off between efficiency and power of the engine, hence yielding more efficiency but slightly smaller power output than the engine operating at maximum power. The numerical values of maximum power and maximum efficient power function are given by $P^{max} = 8.76 \times 10^{-4}$ and $P_\eta^{max} = 5.53 \times 10^{-4}$, respectively. Corresponding efficiencies at maximum power and efficient power functions are given by $\eta^P = 0.593$ and $\eta^{P_\eta} = 0.661$, respectively.

IV. HIGH TEMPERATURE REGIME

Up to now, we have investigated the optimal performance of the engine by numerical techniques only. In order to obtain some analytic results, we will work in the high-temperature limit (classical limit). In order to compare the performance of quantum devices with the classical ones, it is common to practice to work in the high-temperature limit [12, 34, 40, 54–59]. In this case temperature of system is large as compared to energies E_1 and E_2 , i.e. $\beta_l E_i \ll 1$ or $E_i \ll T_l, l = h, 1, c, 2$ and $i = 1, 2$. Similar to our previous consideration about the coupling between the thermal baths, we take $\Gamma_1 = \Gamma_h$

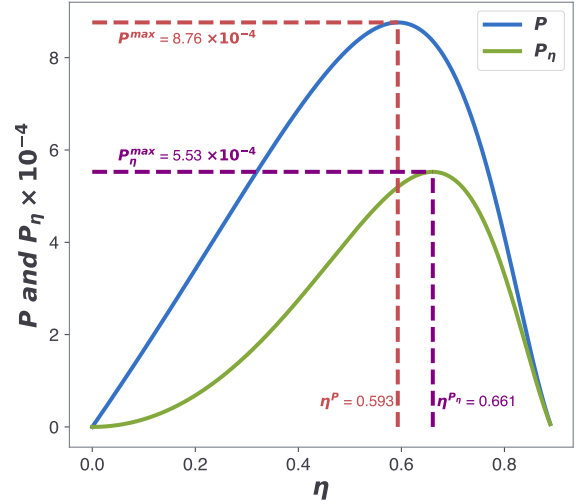


FIG. 4. Figure represents the comparison in between power curve and efficient power optimization varying with the efficiency η . Both the curve has plotted for $E_1 = 10$ and $E_2 = 6$, rest of the parameters are, $\Gamma_h = \Gamma_1 = 0.01, \Gamma_c = \Gamma_2 = 0.001, T_h = 10, T_c = 1$.

and $\Gamma_2 = \Gamma_c$. Applying these constraints, we can obtain the following expressions for Q_1 and Q_2

$$Q_1 = \frac{\Gamma_1}{2(T_1 + T_h)} E_1 (T_h - T_1) \quad (15)$$

$$Q_2 = \frac{\Gamma_2}{2(T_2 + T_c)} E_2 (T_2 - T_c) \quad (16)$$

Further, when $T_h - T_c \ll T_c, T_h + T_1 = 2T_h$ and $T_c + T_2 = 2T_c$, Eqs. (15) and (16) take the following forms

$$Q_1 = k_1 (T_h - T_1), \quad (17)$$

$$Q_2 = k_2 (T_2 - T_c), \quad (18)$$

where $k_1 = \Gamma_1 E_1 / 4T_h$ and $k_2 = \Gamma_2 E_2 / 4T_c$. Both parameter r_1 and r_2 directly depends on coupling parameters, reservoirs temperatures and the energy gaps of the qubits. Thus in the high-temperature limit, the irreversible heat transfer between the reservoirs and the working fluid is governed by Newton's heat transfer law, just as in the case classical endoreversible heat engine.

Using Eqs. (11) and (12) and eliminating T_1 and T_2 in Eqs. (17) and (18), we arrive at the following expressions for the power output, $P = \eta Q_h$, of the engine

$$P^{HT} = \frac{k_1 k_2}{k_1 + k_2} \eta \left(T_h - \frac{T_c}{1 - \eta} \right). \quad (19)$$

The optimization of Eq. (19) with respect to η yields the famous Curzon-Ahlborn efficiency:

$$\eta_{CA} = 1 - \sqrt{\frac{T_c}{T_h}} = 1 - \sqrt{1 - \eta_C} = \frac{\eta_C}{2} + \frac{\eta_C^2}{8} + \frac{\eta_C^3}{16} + \dots, \quad (20)$$

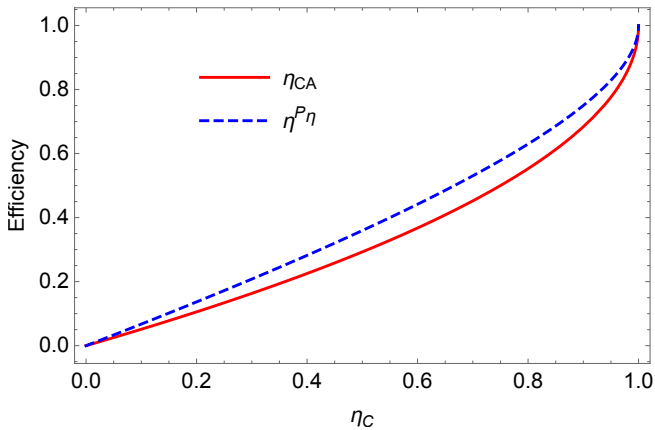


FIG. 5. Plots of efficiency at maximum efficient power, Eq. (22) (dashed blue curve), and efficiency at maximum power, Eq. (20) (solid red curve), as a function of Carnot efficiency η_C for the endoreversible quantum heat engine operating in the high temperature regime.

where we have used the relation $\tau = T_c/T_h = 1 - \eta_C$. Thus, in the high-temperature limit, our quantum endoreversible heat engine operates with the same efficiency at which classical endoreversible heat engine operates. This is expected result as high-temperature limit is considered to be classical limit and in this limit, many models of quantum heat engines and refrigerators operate at CA efficiency [12, 34, 40, 54, 56, 57, 59].

Here, our motivation is to obtain some analytical result in order to compare the performance of the heat engine operating in the maximum power regime to one operating at maximum efficient power function. The expression for the efficient power function can be simply obtained by multiplying Eq. (19) with efficiency η of the engine,

$$P_\eta^{\text{HT}} = \eta P^{\text{HT}} = \frac{k_1 k_2}{k_1 + k_2} \eta^2 \left(T_h - \frac{T_c}{1 - \eta} \right). \quad (21)$$

Optimization of Eq. (21) with respect to η yields the following expression for the efficiency at maximum efficient power function

$$\begin{aligned} \eta^{P_\eta} &= 1 - \frac{1}{4}(1 - \eta_C) \left(1 + \sqrt{1 + \frac{8}{1 - \eta_C}} \right) \\ &= \frac{2\eta_C}{3} + \frac{2\eta_C^2}{27} + \frac{10\eta_C^3}{243} + \dots, \end{aligned} \quad (22)$$

which is exactly same as the efficiency at maximum efficient power of the classical endoreversible [43] and low-dissipation [44] models of heat engine. By comparing Eqs. (20) and (22), we can see that the engine operating at maximum efficient power function is more efficient than the engine at maximum power. We plot Eqs. (20) and (22) in Fig. 5.

A. Fractional loss of power

In this section, we compare the fractional loss of power due to entropy production in our quantum endoreversible heat engine operating at maximum efficient power function to that of operating at maximum power. Power loss due to entropy production is given by: $P_{\text{lost}} = T_2 \dot{S}_{\text{tot}} = \dot{Q}_c - (1 - \eta_C) \dot{Q}_h$. Further using the definitions of power output $P = \dot{Q}_h - \dot{Q}_c$ and efficiency $\eta = P/\dot{Q}_h$, the ratio of power loss to power output can be derived as [50]:

$$R \equiv \frac{P_{\text{lost}}}{P} = \frac{\eta_C}{\eta} - 1. \quad (23)$$

First, we will discuss the fractional power loss in the engine operating under the conditions of maximum efficient power function. Using Eq. (22) in Eq. (23), we have

$$R^{P_\eta} = \frac{1}{4} [\eta_C + \sqrt{(1 - \eta_C)(9 - \eta_C)} - 1], \quad (24)$$

Similarly, we can obtain the corresponding expression for the engine at maximum power by using Eq. (20) in Eq. (23):

$$R^P = \sqrt{1 - \eta_C}. \quad (25)$$

We plot Eqs. (24) and (25) in Fig. 6 as a function of Carnot efficiency η_C . It is clear from Fig. 6 that the

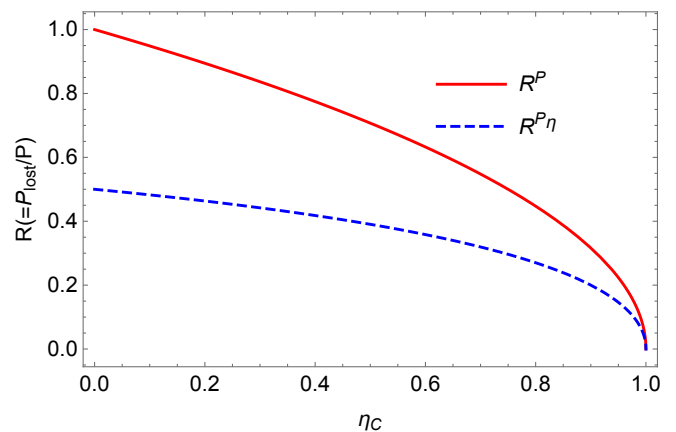


FIG. 6. Comparison of fractional loss of power for two different optimization functions: efficient power function and power output. The lower-lying dashed blue curve (Eq. (24)) represents the case when efficient power function is optimized whereas the upper lying curve (Eq. (25)) represents the case when power output is optimized.

fractional loss of power is much lower when our engine operates in maximum efficient power regime (dashed blue curve in Fig. 6) as compared to the case when our engine operates in maximum power regime (solid red curve in Fig. 6), which in turn implies that engines at maximum efficient power wastes less amount of power thus keeping a check on the environmental pollution and fuel wastage.

Thus, we can conclude that the efficient power is a good objective function from the point of view of environment and fuel conservation.

B. Ratio of power at maximum efficient power to maximum power

Besides the fractional loss of power, another useful quantity to calculate the ratio (R') of power at maximum efficient power to maximum power. The expression for the maximal power can be obtained by substituting Eq. (20) in Eq. (19). We have

$$P_{\text{HT}}^{\text{max}} = \frac{k_1 k_2}{k_1 + k_2} T_h \eta \left(1 - \frac{1 - \eta_C}{1 - \eta} \right) = (1 - \sqrt{1 - \eta_C})^2. \quad (26)$$

Similarly, we can obtain the expression for power at maximum efficient power function by substituting Eq. (22) in Eq. (19):

$$P_{\text{HT}}^{\text{EP}} = \frac{1}{4} \left(-3\sqrt{(1 - \eta_C)(9 - \eta_C)} - 5\eta_C + 9 \right). \quad (27)$$

Dividing Eq. (27) with Eq. (26), we obtain the following expression for the ratio of power at maximum efficient power to maximum power

$$R' = \frac{\left(-3\sqrt{(1 - \eta_C)(9 - \eta_C)} - 5\eta_C + 9 \right)}{4(1 - \sqrt{1 - \eta_C})^2}. \quad (28)$$

For $\eta_C \rightarrow 0$, the ratio $R' = P_{\text{HT}}^{\text{EP}}/P_{\text{HT}}^{\text{max}} = 8/9$, which indicates that at least 88.89% of the maximum power is produced when our engine operates in the maximum efficient power regime, which is a considerable amount since the power loss in maximum efficient power regime is exactly 1/2 (for $\eta_C \rightarrow 0$) of the case when the engine operates at maximum power.

V. STOCHASTIC SIMULATIONS

We studied the thermal fluctuations for quantum endoreversible engine [53]. For stochastic simulations we choose three reference efficiencies $\eta_0 = 0.45$ (where both P and P_η are positive and have small values), $\eta_0 = \eta^P$ (efficiency at maximum power) and $\eta_0 = \eta^{P_\eta}$ (efficiency at maximum efficient power). η is varied randomly around these reference frequencies and we calculate the change in power (ΔP) of the engine for each case. The graphs shows that the power P oscillates randomly around mean P for each case (see Fig. 8). The oscillations are largest for the case with $\eta_0 = 0.45$. However, we are more interested in comparing the the cases when chosen reference efficiencies are $\eta_0 = \eta^P$ and $\eta_0 = \eta^{P_\eta}$. We find that the engine is subjected to relatively larger power fluctuations (orange colored oscillations in Fig. 8) when operating in the maximum efficient power regime as compared to the

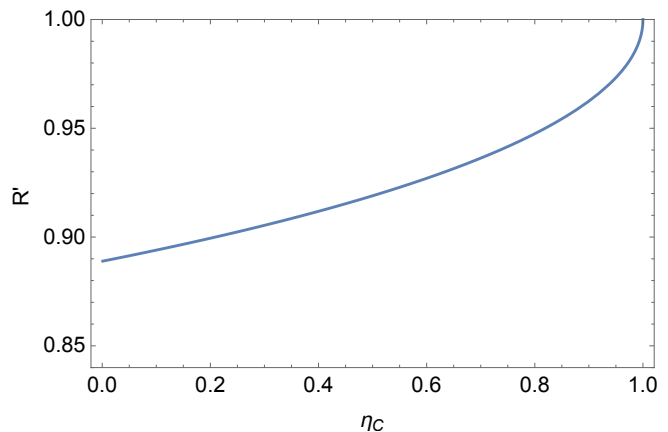


FIG. 7. Ratio R' (Eq. (28)) of the power output at maximum efficient power (Eq. (27)) to the maximum power (Eq. (26)) as a function of Carnot efficiency η_C .

one at maximum power. Thus we conclude that the engine operating in the maximum power regime is the more stable one.

In our simulations, we restrict the change in η to the range $[0.99\eta_0, 1.01\eta_0]$ for all three cases. Table 1 provides numerical values of the dispersion in power for each case.

TABLE I. Mean values and dispersions for the ΔP and ΔP_η at three different reference efficiencies. The data have been obtained by 500 simulations.

Ref.Effi.	$\langle \Delta P \rangle$	σ_P	$\langle \Delta P^\eta \rangle$	σ_{P_η}
0.45	1.51×10^{-5}	1.18×10^{-5}	1.56×10^{-5}	1.18×10^{-5}
η^P	9.99×10^{-7}	1.23×10^{-6}	9.49×10^{-6}	7.35×10^{-6}
η^{P_η}	1.42×10^{-5}	1.20×10^{-5}	1.07×10^{-6}	1.39×10^{-6}

VI. CONCLUSION

In this work, we have investigated the optimal performance of an endoreversible quantum dot heat engine in which irreversible heat transfer between the baths and the working fluid is mediated via qubits. In order to operate the engine in a regime paying equal attention to power production as well as efficiency, we chose efficient power function as our objective function to optimize. First, we numerically studied the optimization of efficient power function by fixing energy gap E_1 of qubit 1 or by fixing energy gap E_2 of qubit 2. Here we learned that unlike classical endoreversible engine, power and efficiency of the quantum endoreversible heat engine are regulated by the microproperties of the qubits. Then we studied the optimal performance of the engine under consideration in the high temperature regime and obtained analytic expression for the efficient at maximum efficient

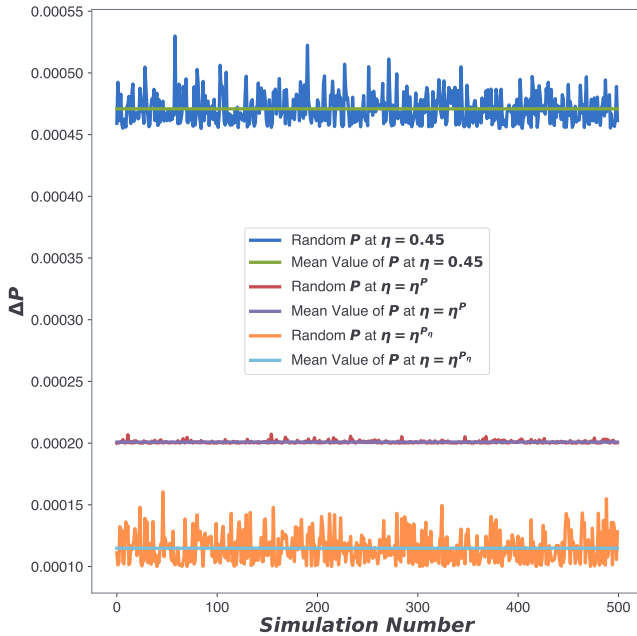


FIG. 8. Fluctuations in power, ΔP , of the engine for the choice of three different reference efficiencies: $\eta_0 = 0.45$, $\eta_0 = \eta^P$ and $\eta_0 = \eta^{P_0}$. The other parameters are fixed at constant values, $E_1 = 10$, $E_2 = 6$, $\Gamma_h = \Gamma_1 = 0.01$, $\Gamma_c = \Gamma_2 = 0.001$, $T_h = 10$, $T_c = 1$.

power function. Additionally, we compared the optimal performance of the quantum endoreversible engine operating at maximum efficient power to that of operating at maximum power. We showed that the fraction loss of power due to entropy production is considerably for the engine at maximum efficient power while at the same time it produces at least 88.89% of the maximum power output. Finally, we also investigated the stability of our engine against thermal fluctuations. We found that the engine operating under the conditions of maximum power is subjected to less fluctuations than the engine operating in the maximum efficient power function, thus rendering it more stable.

VII. ACKNOWLEDGEMENTS

The author gratefully acknowledges the name of Dr. K P Sharma, for his great contribution in resource management.

-
- [1] F. L. Curzon and B. Ahlborn, Am. J. Phys. **43**, 22 (1975).
 - [2] B. Andresen, Angew. Chem. **50**, 2690 (2011).
 - [3] B. Andresen, P. Salamon, and R. S. Berry, Phys. Today **37**, 62 (1984).
 - [4] P. Salamon, J. Nulton, G. Siragusa, T. Andersen, and A. Limon, Energy **26**, 307 (2001).
 - [5] A. de Vos, *Endoreversible Thermodynamics of Solar Energy Conversion* (Oxford University Press, Oxford, UK, 1992).
 - [6] R. S. Berry, V. Kazakov, S. Sieniutycz, Z. Szwast, and A. M. Tsirlin, *Thermodynamic Optimization of Finite-Time Processes* (Wiley, Chichester, UK, 1999).
 - [7] M. H. Rubin and B. Andresen, J. Appl. Phys. **53**, 1 (1982).
 - [8] Z. C. Tu, J. Phys. A **41**, 312003 (2008).
 - [9] M. Esposito, R. Kawai, K. Lindenberg, and C. Van den Broeck, Phys. Rev. Lett. **105**, 150603 (2010).
 - [10] V. Singh and R. S. Johal, J. Stat. Mech. **2018**, 073205 (2018).
 - [11] T. Schmiedl and U. Seifert, Europhys. Lett. **81**, 20003 (2008).
 - [12] O. Abah, J. Roßnagel, G. Jacob, S. Deffner, F. Schmidt-Kaler, K. Singer, and E. Lutz, Phys. Rev. Lett. **109**, 203006 (2012).
 - [13] E. Geva and R. Kosloff, J. Chem. Phys. **97**, 4398 (1992).
 - [14] R. Kosloff, J. Chem. Phys. **80**, 1625 (1984).
 - [15] M. Esposito, K. Lindenberg, and C. Van den Broeck, Phys. Rev. Lett. **102**, 130602 (2009).
 - [16] J. Klatzow, J. N. Becker, P. M. Ledingham, C. Weinzetl, K. T. Kaczmarek, D. J. Saunders, J. Nunn, I. A. Walmsley, R. Uzdin, and E. Poem, Phys. Rev. Lett. **122**, 110601 (2019).
 - [17] M. Josefsson, A. Svilans, A. M. Burke, E. A. Hoffmann, S. Fahlvik, C. Thelander, M. Leijnse, and H. Linke, Nature Nanotechnology **13**, 920 (2018).
 - [18] J. P. S. Peterson, T. B. Batalhão, M. Herrera, A. M. Souza, R. S. Sarthour, I. S. Oliveira, and R. M. Serra, Phys. Rev. Lett. **123**, 240601 (2019).
 - [19] V. Shaghghi, V. Singh, G. Benenti, and D. Rosa, Quantum Science and Technology **7**, 04LT01 (2022).
 - [20] G. Maslennikov, S. Ding, R. Hablützel, J. Gan, A. Roulet, S. Nimmrichter, J. Dai, V. Scarani, and D. Matsukevich, Nat. Commun. **10**, 202 (2019).
 - [21] J. Roßnagel, S. Dawkins, K. Tolazzi, O. Abah, E. Lutz, F. Schmidt-Kaler, and K. Singer, Science **352**, 325 (2016).
 - [22] S. Vinjanampathy and J. Anders, Contemp. Phys. **57**, 545 (2016).
 - [23] S. Bhattacharjee and A. Dutta, The European Physical Journal B **94**, 239 (2021).

- [24] A. T. ÖZDEMİR and Ö. E. MÜSTECAPLIOĞLU, Turk. J. Phys. **44**, 404 (2020).
- [25] R. Alicki and R. Kosloff, in *Thermodynamics in the Quantum Regime* (Springer, 2018) pp. 1–33.
- [26] S. Deffner and S. Campbell, *Quantum Thermodynamics* (Morgan & Claypool Publishers, 2019).
- [27] G. Mahler, *Quantum thermodynamic processes: Energy and information flow at the nanoscale* (Jenny Stanford Publishing, 2014).
- [28] R. Kosloff and A. Levy, Annu. Rev. Phys. Chem. **65**, 365 (2014).
- [29] G. Benenti, G. Casati, K. Saito, and R. S. Whitney, Physics Reports **694**, 1 (2017), fundamental aspects of steady-state conversion of heat to work at the nanoscale.
- [30] N. M. Myers, O. Abah, and S. Deffner, AVS Quantum Science **4**, 027101 (2022).
- [31] A. Auffèves, PRX Quantum **3**, 020101 (2022).
- [32] J. Chen, Z. Yan, G. Lin, and B. Andresen, Energy Convers. and Manage. **42**, 173 (2001).
- [33] F. Angulo-Brown, J. Appl. Phys. **69**, 7465 (1991).
- [34] V. Singh and R. S. Johal, Phys. Rev. E **100**, 012138 (2019).
- [35] V. Singh and R. S. Johal, Entropy **19**, 576 (2017).
- [36] K. Kaur, V. Singh, J. Ghai, S. Jena, and Ö. E. Müstecaplıođlu, Physica A **576**, 125892 (2021).
- [37] V. Singh, S. Singh, O. Abah, and O. E. Müstecaplıođlu, Phys. Rev. E **106**, 024137 (2022).
- [38] A. C. Hernández, A. Medina, J. M. M. Roco, J. A. White, and S. Velasco, Phys. Rev. E **63**, 037102 (2001).
- [39] L. A. Arias-Hernandez, M. A. Barranco-Jiménez, and F. Angulo-Brown, J. Energy Inst. **82**, 223 (2009).
- [40] V. Singh, T. Pandit, and R. S. Johal, Phys. Rev. E **101**, 062121 (2020).
- [41] J. W. Stucki, Eur. J. Biochem. **109**, 269 (1980).
- [42] T. Yilmaz, J. Energy Inst. **79**, 38 (2006).
- [43] Z. Yan and J. Chen, Phys. Lett. A **217**, 137 (1996).
- [44] V. Singh and R. S. Johal, Phys. Rev. E **98**, 062132 (2018).
- [45] V. Singh and R. S. Johal, J. Stat. Mech. **2019**, 093208 (2019).
- [46] Y. Zhang, J. Guo, G. Lin, and J. Chen, J. Non-Equilib. Thermodyn. **42**, 253 (2017).
- [47] J. C. Chimal, N. Sánchez, and P. Ramírez, J. Phys. Conf. Ser. **792**, 012082 (2017).
- [48] N. Sánchez-Salas, J. Chimal-Eguía, and M. Ramírez-Moreno, Physica A: Statistical Mechanics and its Applications **446**, 224 (2016).
- [49] A. Kumari, P. S. Pal, A. Saha, and S. Lahiri, Phys. Rev. E **101**, 032109 (2020).
- [50] V. Singh, Phys. Rev. Research **2**, 043187 (2020).
- [51] N. M. Myers and S. Deffner, Physical Review E **101**, 012110 (2020).
- [52] J. Du, W. Shen, X. Zhang, S. Su, and J. Chen, Phys. Rev. Res. **2**, 013259 (2020).
- [53] J. Fernández, Quantum Science and Technology **7**, 035002 (2022).
- [54] E. Geva and R. Kosloff, Phys. Rev. E **49**, 3903 (1994).
- [55] V. Singh, V. Shaghaghi, Ö. E. Müstecaplıođlu, and D. Rosa, arXiv:2211.08377 (2022).
- [56] E. Geva and R. Kosloff, J. Chem. Phys. **104**, 7681 (1996).
- [57] E. Geva and R. Kosloff, J. Chem. Phys. **96**, 3054 (1992).
- [58] V. Singh and O. E. Müstecaplıođlu, Phys. Rev. E **102**, 062123 (2020).
- [59] B. Lin and J. Chen, Phys. Rev. E **67**, 046105 (2003).